The multiple forms of Bovine Seminal Ribonuclease: structure and stability of a C-terminal swapped dimer.

ARTICLE *in* FEBS LETTERS · OCTOBER 2013

Impact Factor: 3.17 · DOI: 10.1016/j.febslet.2013.10.003 · Source: PubMed

6 AUTHORS, INCLUDING:

Filomena Sica
University of Naples Federico II
93 PUBLICATIONS **1,496** CITATIONS
SEE PROFILE

Antonello Merlino
University of Naples Federico II
129 PUBLICATIONS **1,352** CITATIONS
SEE PROFILE

Irene Russo Krauss
University of Naples Federico II
33 PUBLICATIONS **305** CITATIONS
SEE PROFILE

Delia Picone
University of Naples Federico II
96 PUBLICATIONS **2,190** CITATIONS
SEE PROFILE

FEBS Letters 587 (2013) 3755–3762

FEBS Letters

journal homepage: www.FEBSLetters.org

The multiple forms of bovine seminal ribonuclease: Structure and stability of a C-terminal swapped dimer

Filomena Sica [a,b,c,1], Andrea Pica [a,1], Antonello Merlino [a,b], Irene Russo Krauss [a], Carmine Ercole [a], Delia Picone [a,*]

[a] Department of Chemical Sciences, University of Naples 'Federico II', via Cintia, 80126 Naples, Italy
[b] Institute of Biostructures and Bioimaging, CNR, Via Mezzocannone 16, 80134 Naples, Italy
[c] National Institute Biostructures and Biosystems, Inter-University Consortium, Viale Medaglie d'Oro 305, I-00136 Rome, Italy

ARTICLE INFO

Article history:
Received 13 September 2013
Accepted 7 October 2013
Available online 15 October 2013

Edited by Christian Griesinger

Keywords:
Bovine seminal ribonuclease
C-terminal 3D domain swapping
Multiple swapping
Hinge peptide
Cytotoxic RNase

ABSTRACT

Bovine seminal ribonuclease (BS-RNase) acquires an interesting anti-tumor activity associated with the swapping on the N-terminal. The first direct experimental evidence on the formation of a C-terminal swapped dimer (C-dimer) obtained from the monomeric derivative of BS-RNase, although under non-native conditions, is here reported. The X-ray model of this dimer reveals a quaternary structure different from that of the C-dimer of RNase A, due to the presence of three mutations in the hinge peptide 111–116. The mutations increase the hinge peptide flexibility and decrease the stability of the C-dimer against dissociation. The biological implications of the structural data are also discussed.

Structure summary of protein interactions:
BS-RNase and **BS-RNase** bind by x-ray crystallography (View interaction)
BS-RNase and **BS-RNase** bind by molecular sieving (1, 2)
BS-RNase and **BS-RNase** bind by blue native page (View interaction)

1. Introduction

Three-dimensional domain swapping (3D-DS), a protein interaction mechanism based on the mutual interchange of identical structural elements between identical polypeptide chains, is associated with several biological functions, with either beneficial or toxic consequences for living organisms [1]. It is indeed known that through 3D-DS some proteins acquire new biological functions [2], including selective toxicity for tumour cells [3]. On the other hand 3D-DS has been also associated with amyloid deposits found in some neurodegenerative diseases [4,5]. Very recently, it has been suggested that this mechanism can be widespread in protein folding/unfolding processes [6].

Bovine pancreatic ribonuclease (RNase A) represents a model system for most studies on 3D-DS. Indeed, it is well-known that the first hypothesis of exchange of N-terminal regions was based on biochemical experiments performed on this protein [7]. RNase A was also the first protein showing the possibility to exchange different regions of the polypeptide chain, giving rise to a number of experimental and modelling studies to characterize multimeric assemblies [1]. Later on, the possibility to exchange different regions, or domains, of the polypeptide chain has been reported also for other proteins, like bovine seminal ribonuclease (BS-RNase) [8] and Cyanovirin-N [6], suggesting that this phenomenon may be of more general occurrence.

In the case of RNases, 3D-DS is usually associated with the acquisition of new biological functions beyond their basal enzymatic activity. BS-RNase, a covalent dimeric homologue of RNase A, is isolated as an equilibrium mixture of swapped (M × M) and

Abbreviations: BS-RNase, bovine seminal ribonuclease; D_{ART}-BS, artificial dimer of BS-RNase obtained by incubation in acetic acid of mBS and lyophilisation; D_{ART}-STAA-BS, artificial dimer of STAA-BS-RNase obtained by incubation in acetic acid of STAA-mBS and lyophilisation; DTT, dithiothreitol; IAA, iodoacetamide; L28Q-mBS, L28Q variant of mBS; M × M, covalent swapped isomer of BS-RNase; M = M, covalent unswapped isomer of BS-RNase; mBS, monomeric derivative of BS-RNase with cysteines 31 and 32 either linked to glutathione moieties or alkylated with iodoacetamide; NCD-BS, non-covalent swapped dimer of BS-RNase with cysteines 31 and 32 linked to iodoacetamide, obtained by selective reduction of the swapped isoform and iodoalkylation; PALQ-BS-RNase, P19A/L28Q variant of BS-RNase; PALQ-mBS, P19A/L28Q variant of mBS; R80S-STAA-BS-RNase, R80S variant of STAA-BS-RNase; R80S-STAA-mBS, R80S variant of STAA-mBS; RI, ribonuclease inhibitor; RNase A, bovine pancreatic ribonuclease (EC 3.1.2.27.5); SEC, size-exclusion chromatography; STAA-BS-RNase, G16S/N17T/P19A/S20A variant of BS-RNase; STAA-mBS, G16S/N17T/P19A/S20A variant of mBS

* Corresponding author.
E-mail address: delia.picone@unina.it (D. Picone).
[1] These two authors contributed equally to this work.

0014-5793/$36.00
http://dx.doi.org/10.1016/j.febslet.2013.10.003

unswapped (M = M) isoforms [9] whose subunits are linked by two inter-subunit disulphides formed by Cys31 of one subunit and Cys32 of the other, and vice versa. The M × M form, which through the swapping of the N-terminal α-helices is further stabilized by additional non-covalent interactions between the two subunits, displays a potentially therapeutic cytotoxic activity for tumour cells [10,11]. This feature has been related to the shape [12] and stability [13] of its non-covalent swapped dimeric derivative (NCD-BS), which forms upon selective reduction of the two M × M inter-chain disulphides [14]. Indeed, upon reduction, M × M quaternary structure is preserved and NCD-BS retains the ability to evade the inhibitory binding by Ribonuclease Inhibitor (RI), a protein very abundant in the cytosol of mammalian cells that binds with high affinity RNase A and also other monomeric, pancreatic-like, RNases [15,16]. Studies on dimeric variants of RNase A, obtained by introducing in its sequence residues playing a key role in the acquisition of the BS-RNase 3D-structure, have confirmed the strict relation between antitumor activity and NCD-BS quaternary architecture. Indeed, none of these dimeric variants retains in its non-covalent form a compact quaternary structure able to evade RI [17]. This result well correlates with the much lower cytotoxic activity of these RNase A variants as compared to BS-RNase [18]. Further hints for the design of more powerful mutants can be provided by a deeper, comparative evaluation of the structural and functional features of BS-RNase and RNase A. The two enzymes share more than 80% of the primary structure and a strictly conserved 3D-fold [19], but they have a completely different behaviour with respect to the swapping process. In particular, RNase A swaps either the N- or the C-terminal tail under hard denaturing conditions, forming the N-Dimer and the C-Dimer (hereafter denoted as ND-RNase A and CD-RNase A), respectively [20,21], several trimers [22] and higher size oligomers [23].

In contrast, in BS-RNase the presence of the inter-chain disulphides facilitates the swapping of the N-termini [24]. Interestingly, an analogous behaviour is shown by RNase A variants engineered with the same inter-chains disulphides [18,25].

Up to now, it was believed that the C-swapping was precluded for BS-RNase, due to the presence of a lysine residue replacing asparagine 113 in the C-terminal hinge region (residues 111–116). Very recently we have obtained experimental evidences of the formation of BS-RNase derivatives stabilized by the C-terminal swapping [8]. Here the first clear experimental evidences on the formation of a C-terminal swapped dimer of the monomeric BS-RNase derivatives after incubation in acetic acid and lyophilisation are reported. The crystallographic model of this dimer reveals a quaternary structure different with respect to that adopted by the CD-RNase A. The presence in the crystal structure of only few inter-subunit contacts well explains the low stability of this dimer against dissociation.

2. Materials and methods

2.1. Protein production and purification

Monomeric and dimeric forms of BS-RNase were obtained as previously described [13]. The P19AL28Q (PALQ-BS-RNase) and G16SN17TP19AS20A (STAA-BS-RNase) mutants of BS-RNase were also prepared as already reported [26–28].

The non-covalent dimeric forms of BS-RNase and its mutants were prepared by following two different protocols, i.e., by lyophilisation upon acetic acid incubation of the monomeric derivative iodoalkylated at the cysteines 31 and 32 (mBS) by iodoacetamide (IAA), as reported elsewhere [29], and referred to as "artificial" dimers (D_{ART}), or by selective reduction of the swapped isoform (M × M) of the covalent dimer, as described in detail in Giancola et al. [13], and referred to as NCDs. In both cases the dimers were purified at 4 °C by size exclusion cromatography (SEC) of Sephadex G-75 (1.5 × 72 cm).

Cathodic non-denaturing polyacrylamide gel-electrophoresis was performed at pH 4.5, following the protocol described in Gotte et al. [8].

2.2. Dissociation studies

The dissociation kinetics of the dimers was analysed following the amount of dimeric and monomeric proteins as a function of the incubation time at different temperatures, as previously reported [29]. At regular time intervals, aliquots of the protein samples were loaded on a Superdex 75 HR 10/30 column on FPLC system (Pharmacia, Uppsala, Sweden) equilibrated and eluted in 0.1 M Tris–Cl at pH 7.3 containing 0.13 M NaCl.

2.3. Crystallization and data collection

Solutions of purified D_{ART} of mBS (D_{ART}-BS) and STAA-mBS (D_{ART}-STAA-BS) at concentration 20.0–25.0 mg/ml in 25 mM sodium phosphate at pH 6.7 were used to search for the crystallization conditions. Initial screening was carried out using Hampton Research Crystal Screen 1, Crystal Screen 2, Index, SaltRx and PEG/Ion at 20 °C by the hanging-drop and sitting-drop vapour-diffusion methods. Drops consisting of 0.5 μl protein mixed with an equal volume of precipitating solution were equilibrated against 500 μl of reservoir solution. Best crystals were grown by using a crystallization solution containing 36–40% w/v PEG4K, 0.1 M lithium chloride and 0.1 M sodium cacodylate buffer pH 6.2 or 16–20% w/v PEG35K, 0.2 M lithium chloride, 0.1 M sodium cacodylate buffer pH 6.0 and 3% v/v acetonitrile, for D_{ART}-BS and D_{ART}-STAA-BS, respectively.

X-ray diffraction data were collected at 100 K at the ELETTRA Synchrotron (Trieste, Italy) using a 165 mm CCD detector from MAR-Research. Diffraction data were processed using the program suite HKL2000 [30]. A summary of the indicators commonly used to estimate the quality of datasets is given in Table 1. Pseudo-merohedral twinning (twin law h, -k, -h-l and twin fraction 0.49) was detected using phenix.xtriage from the Phenix suite [31].

2.4. Structure determination and refinement

The structure of D_{ART}-STAA-BS (PDB ID: 4N4C) was solved by molecular replacement using the structure of BS-RNase monomeric derivative (PDB ID: 1N1X) as a search model. The refinement was carried out with REFMAC5 [32] and Phenix [31]. Several alternating cycles of positional refinement, energy minimization, individual temperature factor refinement and manual model building were performed. Model rebuilding was carried out using Coot [33]. The program PROCHECK [34] was used to analyse the quality of the final structure. The refinement statistics are presented in Table 1. Figures were drawn using Pymol [35].

3. Results

3.1. Solution studies

Monomeric samples of BS-RNase with the cysteines 31 and 32 alkylated with IAA were incubated in 40% acetic acid for one hour at room temperature and lyophilised. In a typical experiment, 10 mg of protein were dissolved in 2.0 ml of acetic acid, at a final concentration of 5 mg/ml. After overnight lyophilisation, the protein was dissolved either in 50 mM Tris–Cl buffer at pH 7.3 containing 0.13 M NaCl or 0.2 M phosphate buffer at pH 6.7 and loaded on a G-75 column equilibrated in the same buffer and

Table 1
Data collection and refinement statistics. Values in parentheses refer to the highest resolution shell.

Data collection	
Space group	$P2_1$
Unit-cell parameters (Å, °)	a = 28.80
	b = 79.04
	c = 75.38
	β = 101.05
Resolution range (Å)	20.0–2.48 (2.57–2.48)
Measured reflections	31 997
Unique reflections	9497 (467)
Rmerge (%)	6.3 (19.1)
Mean $I/\sigma(I)$	15.9 (4.5)
Completeness (%)	78.9 (39.0)
Multiplicity	3.4 (2.0)
Twin law	h, $-k$, $-h-l$
Twin fraction	0.49
Refinement statistics	
Resolution limits (Å)	20.0–2.48
R factor (%)	17.0
R_{free} (%)	18.6
Number of reflections used in the refinement	8385
Number of reflections used for R_{free} calculation	420
No. of protein atoms	1889
No. of ions	2
No. of water molecules	35
Average B	
Protein, overall (Å^2)	16.4
Solvent atoms (Å^2)	14.3
Rmsd bond lengths (Å)	0.009
Rmsd bond angles (°)	1.289
Ramachandran statistics	
Favoured region (%)	93.6
Allowed region (%)	5.20
Outliers (%)	1.20

eluted at 4 °C. The chromatographic pattern is reported in Fig. 1 (dashed line). Peak integration revealed that more than 60% of the protein is eluted as monomer (indicated as M), whilst the remaining part corresponds to aggregated forms of different size, although the relative amount of each aggregate varied slightly with the elution buffer. From the elution volume it is possible to calculate that the first peak corresponds to the size of a tetramer, the second (indicated as T_{ART}) to the size of a trimer, and the third (indicated as D_{ART}) to the size of a dimer. The remaining part, equivalent roughly to the 10% of the total, corresponds to higher size aggregates. The dimer accounts for about 20–25% of the total protein amount.

A similar experiment was performed on the STAA-mBS mutant, obtaining the chromatographic profile also reported in Fig. 1 (solid line), which closely resembles the one obtained with the parent (wild-type) protein, except for the slightly higher amount of aggregates. Very similar results were obtained with other BS-RNase mutants, in which residues having key roles in the swapping phenomenon were substituted with the corresponding ones of RNase A and which have a different behaviour with respect to the swapping of the N-terminal ends, i.e., R80S-STAA-mBS [27] and PALQ-mBS [28]. The elution profile of PALQ-mBS is also shown in Fig. 1 as an example (dotted line).

The fractions corresponding to the artificial dimers of both BS-RNase and STAA-BS-RNase were pooled and a small amount of these protein samples was loaded on a polyacrylamide gel run under native conditions (pH 4.5). Aliquots of BS-RNase and of NCD-BS together with the monomeric forms of BS-RNase and STAA-BS-RNase (mBS and STAA-mBS) were also loaded on the gel (Fig. 2). The analysis of the gel indicated clearly that BS-RNase and NCD-BS (lanes 3 and 4) are characterized by a single band. On the contrary, both the artificial dimers (lanes 5 and 6) showed the presence of a significant amount of the corresponding monomeric forms (lanes 1 and 2), which necessarily had to be produced upon dissociation of the dimeric species after the gel-filtration and even while running the gel. Interestingly, the comparison of lanes 3 and 4 with 5 and 6 indicates that the artificial dimers migrate on the gel with a mobility very close to that of NCD-BS, thus suggesting the presence of a single dimeric form even in the samples prepared by acetic acid lyophilisation, in contrast with the results obtained for RNase A. It is indeed well known that the two dimers formed when RNase A is subjected to the same treatment can be separated by cathodic gel-electrophoresis [36].

The fast dissociation of the artificial dimers indicated by the gel-electrophoresis prompted a further characterization of their stability in solution. Therefore, a comparison of the dissociation processes of the NCD forms of BS-RNase and STAA-BS-RNase with the corresponding artificial dimers, i.e., D_{ART}-BS and D_{ART}-STAA-BS has been performed. The proteins have been incubated at 37 °C and, at regular time intervals, aliquots corresponding to 0.2 mg of each sample were loaded on Superdex 75 to evaluate the relative amount of dimer and monomer. Surprisingly, the kinetic stability of the two artificial dimers was found significantly lower than that of the corresponding NCD forms: the $t_{1/2}$ of the artificial dimers were 1.5 h for D_{ART}-BS and 0.6 h for D_{ART}-STAA-BS, while the values of the partner NCDs, measured in the same experimental conditions, were 6.1 h and 2.2 h, respectively (Table 2). These results suggest that the two dimeric forms obtained in different experimental conditions, i.e., the NCDs and the artificial dimers, have

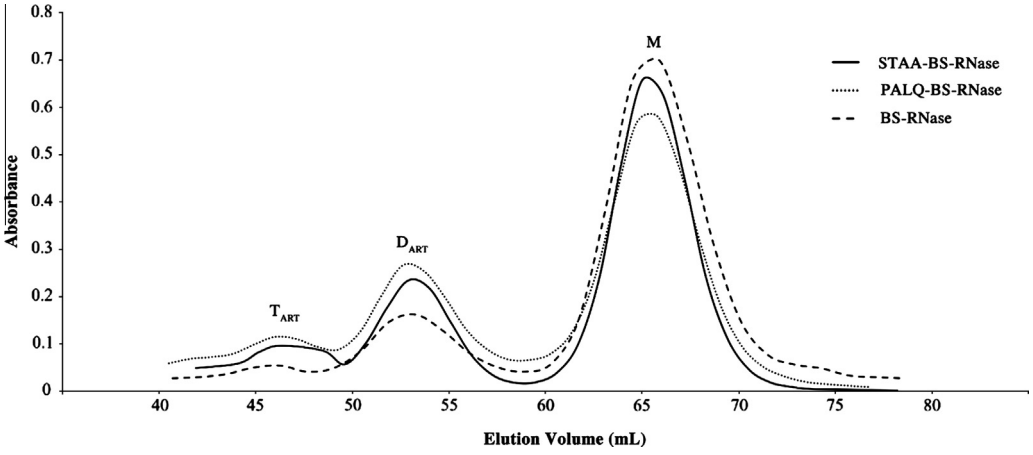

Fig. 1. Chromatographic pattern of a gel-filtration on Sephadex G-75 upon acetic acid incubation and lyophilisation of the monomeric derivatives of STAA-BS-RNase, PALQ-BS-RNase, and BS-RNase.

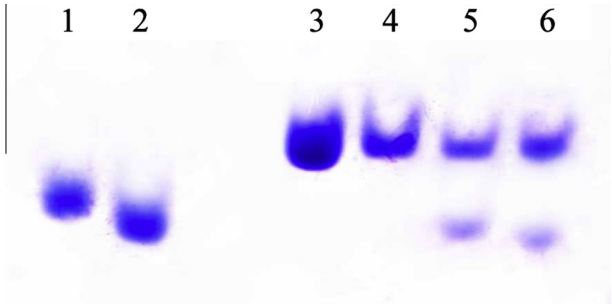

Fig. 2. Poly-acrylamide gel-electrophoresis under native conditions of the dimeric forms obtained by incubation in acetic acid followed by lyophilisation of the monomeric derivatives of BS-RNase and STAA-BS-RNase (mBS and STAA-mBS) (lanes 5 and 6). The corresponding monomeric forms (lanes 1 and 2), together with BS-RNase (lane 3) and NCD-BS, obtained by selective reduction of the swapped dimer (lane 4), are also reported for comparison.

Table 2
Half-live times $t_{1/2}$ of dimers from dissociation experiments.

	$t_{1/2}$ (h)	E_a (kcal/mol)
NCD-BS	6.1	–
D_{ART}-BS	1.5	–
NCD-STAA-BS	2.2	92.2
D_{ART}-STAA-BS	0.6	56.8

different quaternary structures. Interestingly, the two variants conserved the same relative stability, with the STAA mutant displaying the faster dissociation rate.

A deeper comparison of the behaviour of NCD and D_{ART} dimers has been performed for the STAA-BS-RNase variant, by measuring the dissociation rate at different temperatures. Straight lines were obtained at all the temperature explored (in the range 15–37 °C), confirming the homogeneity of all the protein samples. Furthermore, the Arrhenius plot of the kinetic constants allowed the calculation of the activation energy of the dissociation process, reported in Table 2, which were 92.2 kcal/mol for NCD and 56.8 kcal/mol for D_{ART} respectively.

These results clearly indicated that NCD and D_{ART} dimers have different quaternary structures, and consequently different stabilities, in solution. The fast dissociation of the artificial dimers prevented any further characterization in solution.

3.2. Crystal growth

The extensive search for crystallization conditions has produced different results in the case of the native enzyme and of its STAA variant. Crystals of D_{ART}-BS grew in a very short time (about 12 h), showed an even shorter lifetime (about 10 h), were quite disordered and their diffraction power decayed after few minutes of X-ray exposure. As a consequence, only few diffraction images were recorded. In the case of D_{ART}-STAA-BS, the higher stability of the crystals allowed a complete X-ray diffraction data collection at 2.48 Å resolution. Unfortunately, in addition to their low diffraction power, essentially due to their high solvent content (about 60%), crystals are twinned by pseudo-merohedry (see Section 2).

3.3. Crystallographic analysis

The features of D_{ART}-STAA-BS crystals (low diffraction power and twinning) made both solution and refinement processes not trivial. The structure was solved by molecular replacement using the BS-RNase monomer as a search model (PDB code: 1N1X). The asymmetric unit contains two protein chains, whose position and orientation are compatible with the swapping of their C-terminal arms. The structure was refined at 2.48 Å resolution to a *R value* of 0.170 (R_{free} = 0.186) and the final model includes 1889 protein atoms, 2 phosphate ions and 35 water molecules. The average B-factor computed for all protein atoms is 16.4 Å^2. A full list of refinement statistics is reported in Table 1, and the crystallographic structure of D_{ART}-STAA-BS is reported in Fig. 3.

The quality of the electron density maps allowed a detailed description of nearly the whole molecule. The two chains share an almost identical structure, as judged from their very low root mean square deviation (rmsd) of 0.4 Å (rmsd calculated for main chain atoms excluding residues 111–116). No major topological variation has been found in the common ribonuclease fold adopted by each subunit (defined as the structural unit formed by residue 1–110 of one chain, the core of the protein, and residues 117–124 of the other chain, the swapped domain). Indeed the rmsd between one of the two subunits and the monomeric enzyme (PDB code: 1N1X) is ~0.7 Å (rmsd calculated for main chain atoms of residues 1–110 and 117–124). A phosphate ion is bound to each composite catalytic site stabilizing the dimer by mimicking the enzyme substrate, as typically observed in several other ribonuclease structures [12,21,29,37,38].

The electron density associated with the hinge region (residues 111–116), which connects the swapped domain to the rest of the protein, is continuous for the A subunit (Fig. 4B) but less well defined in the case of the B subunit. The conformation of segment 111A–116A is stabilized by a strong intra-chain H-bond between the side chains of K113 and S115 (Fig. 4). None of the two hinge peptides adopts the β-sheet conformation shown by the same regions in the CD-RNase A structure (Fig. 5). In the latter, the N113 enforces the hydrogen bonding network in the β-sheet alignment of the two

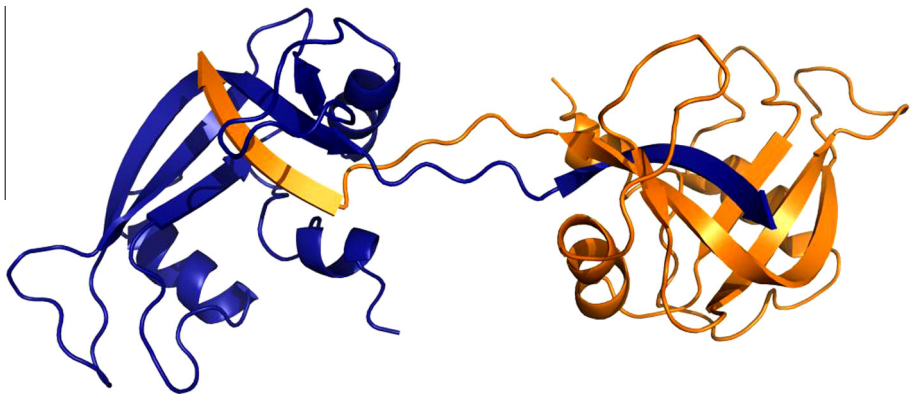

Fig. 3. Crystallographic structure of D_{ART}-STAA-BS represented as cartoon. The two chains are coloured differently to highlight the C-terminal swapping.

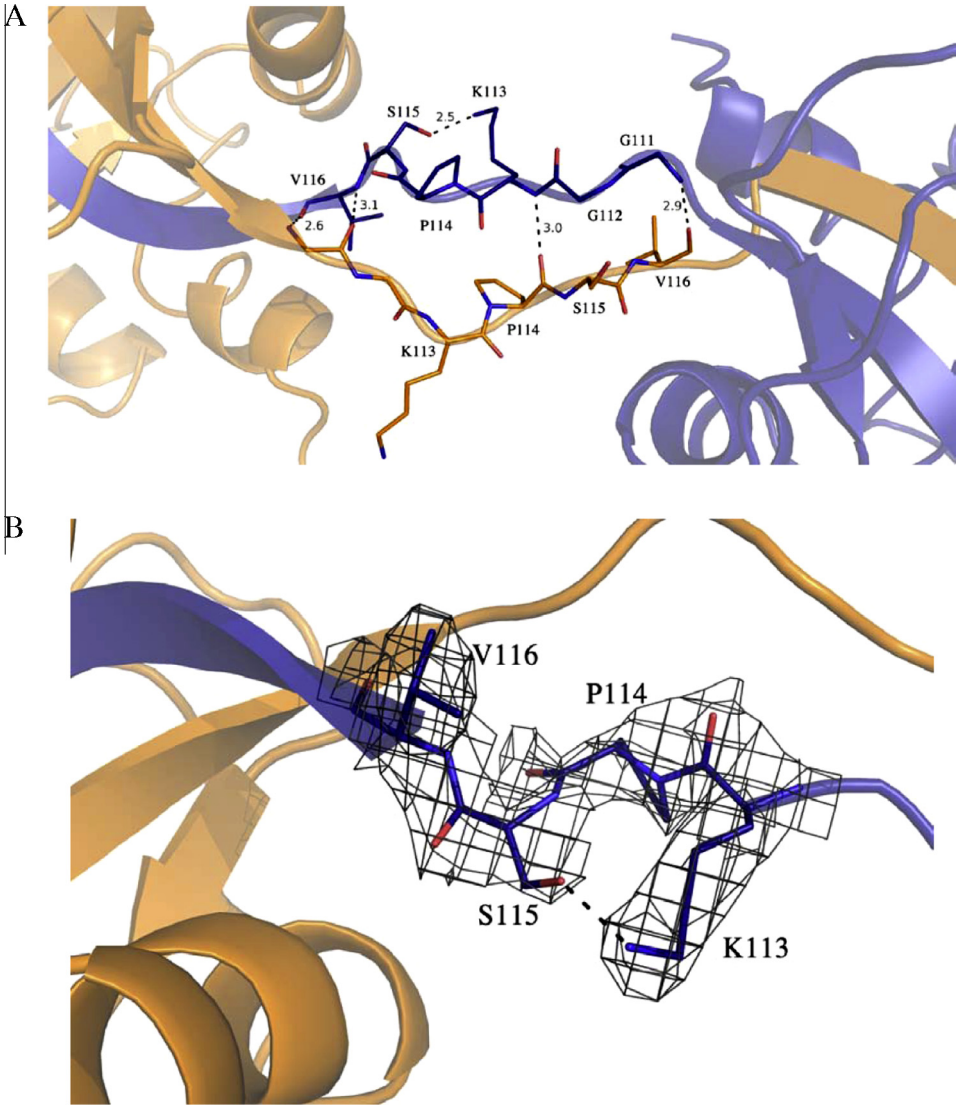

Fig. 4. (A) Structure of the hinge peptides of D_{ART}-STAA-BS. Distances are reported in Angstrom. Chain A is coloured blue while chain B is coloured orange. (B) $2F_o - F_c$ electron density map of the hinge peptide of chain A contoured at 1.0 σ.

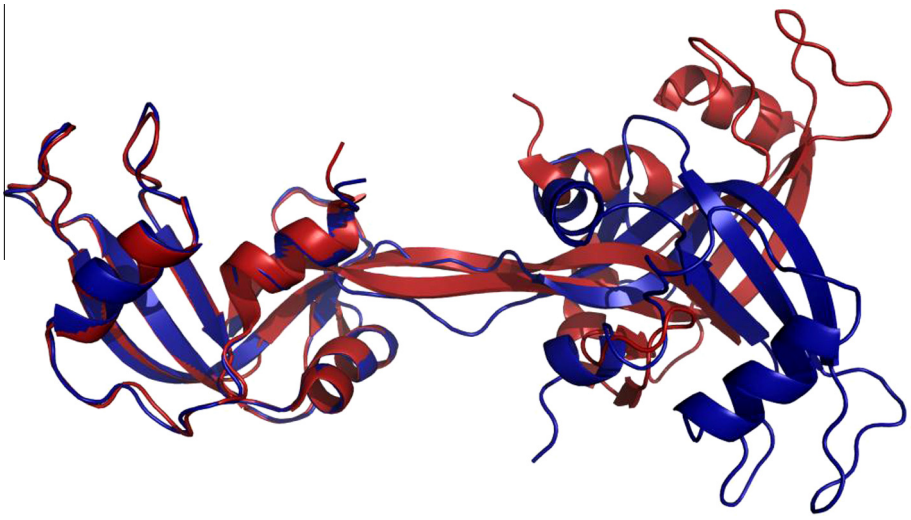

Fig. 5. Comparison of the overall structures of D_{ART}-STAA-BS (in blue) and CD-RNase A (in red). Only one subunit (composed by residues 1–110 of chain A and residues 117–124 of chain B) of each dimer has been superimposed; a further 150° rotation is needed to best superpose the second structural unit (residues 1–110 of chain B and residues 117–124 of chain A) of the two dimers.

hinge peptides. In the seminal enzyme the presence of a lysine in that position replaces the stabilizing H-bond with a positive charge repulsion. Moreover, the mutations of E111 with G and Y115 with S confer a much higher flexibility to this region in the structure of the C-Dimer of BS-RNase when compared to CD-RNase A, as indicated by the low definition of the electron density of the B subunit hinge peptide, and thus to the whole swapped dimer. As a consequence, in the case of D_{ART}-STAA-BS there is a decrease in the number of the inter-hinge contacts. It has to be noticed that in the case of the C-swapped dimers of both RNases the only additional interactions formed upon domain-swapping (open interface) involve residues of the hinge peptides. In particular, the swapped dimer is stabilized by the burying at the interface between the two hinge peptides of an area of about 390 and 520 Å^2 for D_{ART}-STAA-BS and CD-RNase A, respectively. The peculiar structural features of the hinge segments produce a quaternary organization of D_{ART}-STAA-BS very different from that of CD-RNase A [21]. Indeed, after superimposition of one subunit of each dimer, a further rotation of about 150° has to be applied in order to best overlap the second subunits (Fig. 5).

4. Discussion

The comparison of the swapping properties of RNase A and BS-RNase can provide interesting clues to investigate the 3D-DS mechanism and its functional implications. Despite the high similarity of their amino acid sequence (more than 80% identity) the two proteins have a completely different behaviour with respect to the swapping [12,14,17,26,29]. The N-terminal swapping mechanism in both systems has already been studied [12,14,17,26,29] and the residues playing a key role in the process have been identified [17].

This paper represents the first detailed analysis of the C-terminal arm swapping in the bovine seminal enzyme. In particular, we report the 3D structure of the single dimer that is formed when the monomeric derivative of STAA-BS-RNase is incubated in 40% acetic acid and lyophilised, and the characterization of its stability against dissociation. These data provide a further evidence of the distinct properties between RNase A and BS-RNase. The crystallographic model of D_{ART}-STAA-BS shows that in BS-RNase the exchange of the C-terminal arms between the two subunits

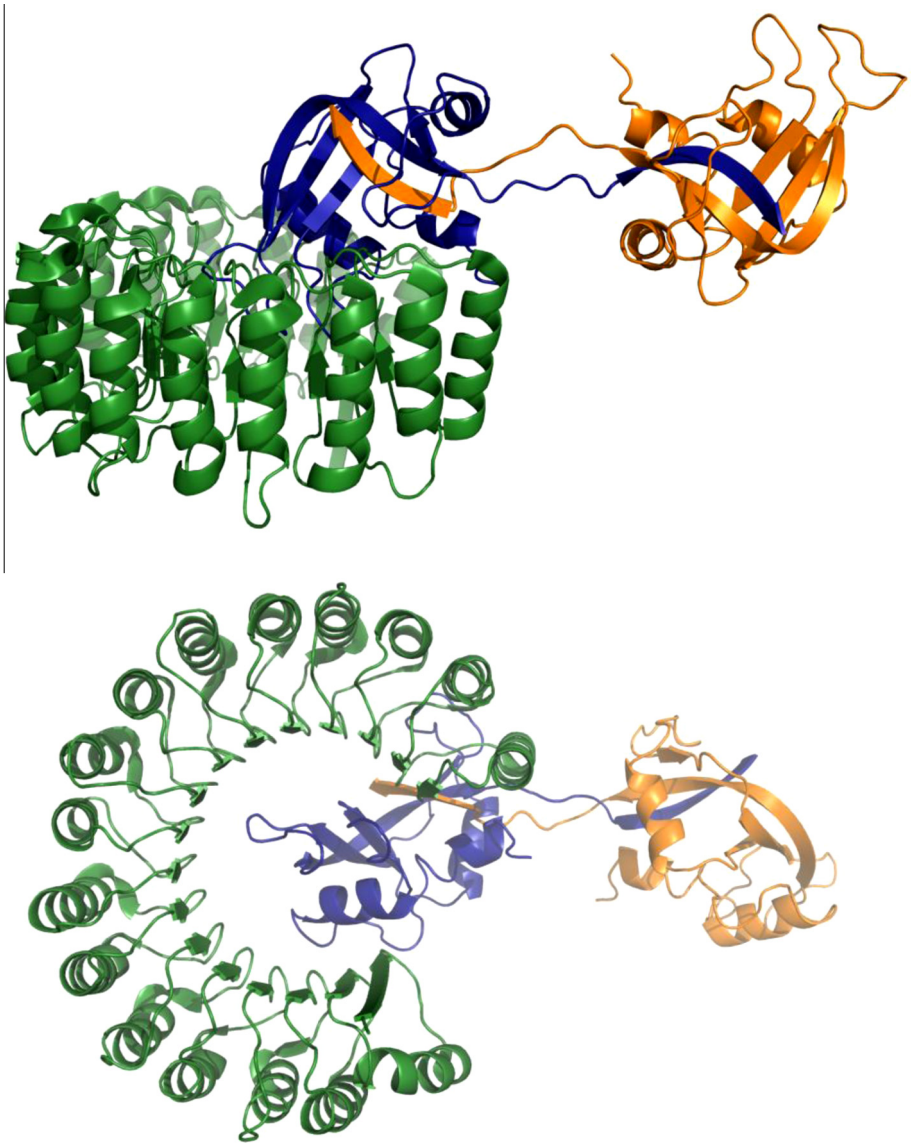

Fig. 6. Putative model of the complex between the ribonuclease inhibitor (PDB code: 1Z7X) and D_{ART}-STAA-BS in two different orientations.

produces a dimer that adopts a different quaternary organization when compared to that observed in the case of CD-RNase A, namely the RNase A dimer swapping the same structural elements. This variation is mainly due to the change in the structure adopted by the hinge peptides (111–116) of the two enzymes. In particular, in D_{ART}-STAA-BS the β-sheet organization found in the CD-RNase A structure seems to be hampered by the unfavourable interaction between two lysine residues at position 113. On this respect, it is worth to mention here that the lyophilisation from acetic acid of the monomeric variant of BS-RNase where lysine 113 was replaced with asparagine, i.e., the residue present at the same position in RNase A, produces an higher amount of the C-terminal swapped dimer and other multimers in comparison with the wild-type enzyme [8]. The substitution also results in an increased stability of the oligomeric forms [8]. The other two substitutions present in the hinge peptide of the seminal enzyme, E111→G and Y115→S, confer a high conformational flexibility to this region, facilitating the dissociation of the dimer in solution. All these experimental data confirm the important role that in the 3D-DS phenomenon is played by the hinge region [4,38,39], the only structural element that in a swapping process undergoes a rather large conformational rearrangement.

Interestingly, no traces of a N-terminal swapped (artificial) dimer of BS-RNase and STAA-BS-RNase have been found in our experimental conditions. This unexpected result could be due to a quick dissociation of the dimer or to a very high energy barrier separating the monomer from the NCD form. The experimental conditions, in turn, could push the refolding pathway towards the formation of the C-swapped dimer, which is formed more easily despite its low stability, and represents the highest quantity (about 16%) among the aggregated forms recovered from SEC. The different swapping behaviour of the bovine seminal and pancreatic enzymes has most likely to be ascribed to the sequence mutations.

Like in the case of RNase A, some higher size aggregates are also formed by lyophilisation from acetic acid, although in this paper we focused only on the dimer. The structures of these aggregates are still unknown, therefore the presence of N-terminal swapping cannot be excluded. At any rate, the characterization of the multimers obtained when the native, dimeric BS-RNase is treated in the same conditions [8] suggests the occurrence of N-terminal swapping as well.

As far as the biological implications are concerned, unfortunately the fast dissociation of the artificial dimers in solution precluded a functional characterization, although it is possible to foresee that they should be devoid of any significant antitumor function. Modelling studies indicate indeed that the X-ray structure of D_{ART}-STAA-BS fits nicely in the RI cavity, as shown in Fig. 6, thus reducing the high potential associated with 3D-DS. Based on these considerations, it can be inferred that the C-swapping of BS-RNase represents an unfavourable event with respect to the N-swapping, therefore the substitutions of E111, N113, and Y115 of RNase A with G111, K113 and S115 in BS-RNase should be considered a favourable event in the evolution, since they reduce the effects of C-terminal swapping. Finally, these data enforce the role of the disulphide bridges linking the two subunits of BS-RNase, which giving the right orientation to the subunits prepare the N-terminal swapping [24] and facilitate its occurrence under mild, physiological conditions.

Acknowledgments

The authors thank Lelio Mazzarella for his very helpful comments and suggestions during the development of this work.

References

[1] Liu, Y. and Eisenberg, D. (2002) 3D domain swapping: as domains continue to swap. Protein Sci. 11, 1285–1299.
[2] Vitagliano, L., Adinolfi, S., Sica, F., Merlino, A., Zagari, A., et al. (1999) A potential allosteric subsite generated by domain swapping in bovine seminal ribonuclease. J. Mol. Biol. 293, 569–577.
[3] Youle, R.J. and D'Alessio, G. (1997) Antitumor RNases in: Ribonucleases: Structures and Functions. (G. D'Alessio and J.F. Riordan Eds.), Academic Press, New York, 491-514.
[4] Sambashivan, S., Liu, Y., Sawaya, M.R., Gingery, M. and Eisenberg, D. (2005) Amyloid-like fibrils of ribonuclease A with three-dimensional domain-swapped and native-like structure. Nature 437, 266–269.
[5] Bennett, M.J., Sawaya, M.R. and Eisenberg, D. (2006) Deposition diseases and 3D domain swapping. Structure 14, 811–824.
[6] Koharudin, L.M., Liu, L. and Gronenborn, A.M. (2013) Different 3D domain-swapped oligomeric cyanovirin-N structures suggest trapped folding intermediates. Proc. Natl. Acad. Sci. USA 110, 7702–7707.
[7] Crestfield, A.M., Stein, W.H. and Moore, S. (1963) On the preparation of bovine pancreatic ribonuclease A. J. Biol. Chem. 238, 618–621.
[8] Gotte, G., Mahmoud Helmy, A., Ercole, C., Spadaccini, R., Laurents, D.V., et al. (2012) Double domain swapping in bovine seminal RNase: formation of distinct N- and C-swapped tetramers and multimers with increasing biological activities. PLoS One 7, e46804.
[9] Piccoli, R., Tamburrini, M., Piccialli, G., Di Donato, A., Parente, A., et al. (1992) The dual-mode quaternary structure of seminal RNase. Proc. Natl. Acad. Sci. USA 89, 1870–1874.
[10] Matousek, J. (1973) The effect of bovine seminal ribonuclease (AS RNase) on cells of Crocker tumour in mice. Experientia 29, 858–859.
[11] Kim, J.S., Soucek, J., Matousek, J. and Raines, R.T. (1995) Structural basis for the biological activities of bovine seminal ribonuclease. J. Biol. Chem. 270, 10525–10530.
[12] Merlino, A., Ercole, C., Picone, D., Pizzo, E., Mazzarella, L., et al. (2008) The buried diversity of bovine seminal ribonuclease: shape and cytotoxicity of the swapped non-covalent form of the enzyme. J. Mol. Biol. 376, 427–437.
[13] Giancola, C., Ercole, C., Fotticchia, I., Spadaccini, R., Pizzo, E., et al. (2011) Structure–cytotoxicity relationships in bovine seminal ribonuclease: new insights from heat and chemical denaturation studies on variants. FEBS J. 278, 111–122.
[14] Sica, F., Di Fiore, A., Merlino, A. and Mazzarella, L. (2004) Structure and stability of the non-covalent swapped dimer of bovine seminal ribonuclease: an enzyme tailored to evade ribonuclease protein inhibitor. J. Biol. Chem. 279, 36753–36760.
[15] Kobe, B. and Deisenhofer, J. (1996) Mechanism of ribonuclease inhibition by ribonuclease inhibitor protein based on the crystal structure of its complex with ribonuclease A. J. Mol. Biol. 264, 1028–1043.
[16] Kobe, B. and Deisenhofer, J. (1993) Crystal structure of porcine ribonuclease inhibitor, a protein with leucine-rich repeats. Nature 366, 751–756.
[17] Merlino, A., Russo Krauss, I., Perillo, M., Mattia, C.A., Ercole, C., et al. (2009) Toward an antitumor form of bovine pancreatic ribonuclease: the crystal structure of three noncovalent dimeric mutants. Biopolymers 91, 1029–1037.
[18] Ercole, C., Colamarino, R.A., Pizzo, E., Fogolari, F., Spadaccini, R., et al. (2009) Comparison of the structural and functional properties of RNase A and BS-RNase: a stepwise mutagenesis approach. Biopolymers 91, 1009–1017.
[19] Spadaccini, R., Ercole, C., Gentile, M.A., Sanfelice, D., Boelens, R., et al. (2012) NMR studies on structure and dynamics of the monomeric derivative of BS-RNase: new insights for 3D domain swapping. PLoS One 7, e29076.
[20] Liu, Y., Hart, P.J., Schlunegger, M.P. and Eisenberg, D. (1998) The crystal structure of a 3D domain-swapped dimer of RNase A at a 2.1-A resolution. Proc. Natl. Acad. Sci. USA 95, 3437–3442.
[21] Liu, Y., Gotte, G., Libonati, M. and Eisenberg, D. (2001) A domain-swapped RNase A dimer with implications for amyloid formation. Nat. Struct. Biol. 8, 211–214.
[22] Liu, Y., Gotte, G., Libonati, M. and Eisenberg, D. (2002) Structures of the two 3D domain-swapped RNase A trimers. Protein Sci. 11, 371–380.
[23] Cozza, G., Moro, S. and Gotte, G. (2008) Elucidation of the ribonuclease A aggregation process mediated by 3D domain swapping: a computational approach reveals possible new multimeric structures. Biopolymers 89, 26–39.
[24] Mazzarella, L., Vitagliano, L. and Zagari, A. (1995) Swapping structural determinants of ribonucleases: an energetic analysis of the hinge peptide 16–22. Proc. Natl. Acad. Sci. USA 92, 3799–3803.
[25] Di Donato, A., Cafaro, V. and D'Alessio, G. (1994) Ribonuclease A can be transformed into a dimeric ribonuclease with antitumor activity. J. Biol. Chem. 269, 17394–17396.
[26] Picone, D., Di Fiore, A., Ercole, C., Franzese, M., Sica, F., et al. (2005) The role of the hinge loop in domain swapping. The special case of bovine seminal ribonuclease. J. Biol. Chem. 280, 13771–13778.
[27] Ercole, C., Spadaccini, R., Alfano, C., Tancredi, T. and Picone, D. (2007) A new mutant of bovine seminal ribonuclease with a reversed swapping propensity. Biochemistry 46, 2227–2232.
[28] Ercole, C., Avitabile, F., Del Vecchio, P., Crescenzi, O., Tancredi, T., et al. (2003) Role of the hinge peptide and the intersubunit interface in the swapping of N-termini in dimeric bovine seminal RNase. Eur. J. Biochem. 270, 4729–4735.

[29] Merlino, A., Picone, D., Ercole, C., Balsamo, A. and Sica, F. (2012) Chain termini cross-talk in the swapping process of bovine pancreatic ribonuclease. Biochimie 94, 1108–1118.
[30] Otwinowski, Z. and Minor, W. (1997) Processing of X-ray diffraction data collected in oscillation mode in: Methods Enzymol. (Carter, Charles W. Jr.Jr., Ed.), pp. 307–326, Academic Press.
[31] Adams, P.D., Afonine, P.V., Bunkoczi, G., Chen, V.B., Davis, I.W., et al. (2010) PHENIX: a comprehensive Python-based system for macromolecular structure solution. Acta Crystallogr., D 66, 213–221.
[32] Vagin, A.A., Steiner, R.A., Lebedev, A.A., Potterton, L., McNicholas, S., et al. (2004) REFMAC5 dictionary: organization of prior chemical knowledge and guidelines for its use. Acta Crystallogr., D 60, 2184–2195.
[33] Emsley, P., Lohkamp, B., Scott, W.G. and Cowtan, K. (2010) Features and development of Coot. Acta Crystallogr., D 66, 486–501.
[34] Laskowski, R.A., MacArthur, M.W., Moss, D.S. and Thornton, J.M. (1993) PROCHECK: a program to check the stereochemical quality of protein structures. J. Appl. Crystallogr. 26, 283–291.
[35] Schrodinger, LLC (2010) The PYMOL Molecular Graphics System, Version 1.3r1. PYMOL http://wwwpymolorg.
[36] Gotte, G., Bertoldi, M. and Libonati, M. (1999) Structural versatility of bovine ribonuclease A. Distinct conformers of trimeric and tetrameric aggregates of the enzyme. Eur. J. Biochem. 265, 680–687.
[37] Merlino, A., Mazzarella, L., Carannante, A., Di Fiore, A., Di Donato, A., et al. (2005) The importance of dynamic effects on the enzyme activity: X-ray structure and molecular dynamics of onconase mutants. J. Biol. Chem. 280, 17953–17960.
[38] Merlino, A., Avella, G., Di Gaetano, S., Arciello, A., Piccoli, R., et al. (2009) Structural features for the mechanism of antitumor action of a dimeric human pancreatic ribonuclease variant. Protein Sci. 18, 50–57.
[39] Pica, A., Merlino, A., Buell, A.K., Knowles, T.P.J., Pizzo, E., et al. (2013) Three-dimensional domain swapping and supramolecular protein assembly: insights from the X-ray structure of a dimeric swapped variant of human pancreatic RNase. Acta Crystallogr. D 69, 2116–2123.